Remote Sensing of Environment 113 (2009) 2118–2129

Contents lists available at ScienceDirect

Remote Sensing of Environment

journal homepage: www.elsevier.com/locate/rse

A novel ocean color index to detect floating algae in the global oceans

Chuanmin Hu *

College of Marine Science, University of South Florida, 140 Seventh Avenue, South, St. Petersburg, FL 33701, United States

ARTICLE INFO

Article history:
Received 27 December 2008
Received in revised form 15 May 2009
Accepted 23 May 2009

Keywords:
Floating Algae Index (FAI)
NDVI
EVI
Algal bloom
Enteromorpha prolifera
Sargassum spp.
Porphyra yezoensis
Atmospheric correction
Remote sensing
Ocean color
Climate data record

ABSTRACT

Various types of floating algae have been reported in open oceans and coastal waters, yet accurate and timely detection of these relatively small surface features using traditional satellite data and algorithms has been difficult or even impossible due to lack of spatial resolution, coverage, revisit frequency, or due to inherent algorithm limitations. Here, a simple ocean color index, namely the Floating Algae Index (FAI), is developed and used to detect floating algae in open ocean environments using the medium-resolution (250- and 500-m) data from operational MODIS (Moderate Resolution Imaging Spectroradiometer) instruments. FAI is defined as the difference between reflectance at 859 nm (vegetation "red edge") and a linear baseline between the red band (645 nm) and short-wave infrared band (1240 or 1640 nm). Through data comparison and model simulations, FAI has shown advantages over the traditional NDVI (Normalized Difference Vegetation Index) or EVI (Enhanced Vegetation Index) because FAI is less sensitive to changes in environmental and observing conditions (aerosol type and thickness, solar/viewing geometry, and sun glint) and can "see" through thin clouds. The baseline subtraction method provides a simple yet effective means for atmospheric correction, through which floating algae can be easily recognized and delineated in various ocean waters, including the North Atlantic Ocean, Gulf of Mexico, Yellow Sea, and East China Sea. Because similar spectral bands are available on many existing and planned satellite sensors such as Landsat TM/ETM+ and VIIRS (Visible Infrared Imager/Radiometer Suite), the FAI concept is extendable to establish a long-term record of these ecologically important ocean plants.

1. Introduction

Beginning with the Coastal Zone Color Scanner (1978–1986), all satellite ocean color sensors have been designed to measure the spectral water-leaving radiance or surface reflectance in order to derive concentrations of the various water constituents including chlorophyll-*a*. Indeed, the phrase "ocean color" is often regarded as equivalent to chlorophyll-*a* concentration. Significant progress has been made in the past two decades, through modern sensor development, calibration, validation, and algorithm improvement, to derive a suite of the ocean's bio-optical properties such as chlorophyll-*a* concentration, absorption coefficient of colored dissolved organic matter (CDOM), diffuse attenuation coefficient, and euphotic depth (Yentsch, 1960, 1983; Morel & Prieur, 1977; Austin & Petzold, 1981; Gordon & Morel, 1983; Sathyendranath et al., 1989; Cullen et al., 1997; Gordon, 1997; O'Reilly et al., 2000; Maritorena et al., 2002; Lee et al., 2002, 2005; McClain et al., 2004; IOCCG, 2005; others). Algorithms have also been developed to detect some phytoplankton functional groups due to their unique optical properties, including Coccolithophores (Brown & Yoder, 1994; Gordon et al., 2001), cyanobacteria *Trichodesimum* spp. (Subramaniam et al., 2002), cyanobacteria *Nodularia spumigena* (Kahru et al., 2007), diatoms (Sathyendranath et al., 2004), harmful algae (Cannizzaro et al., 2008), and other groups (Morel et al., 1993; Alvain et al., 2005). Consequently, in addition to the application of the science-quality ocean color data in global and regional biogeochemical studies, ocean color data have also been used to monitor and study harmful algal blooms (HABs), sediment resuspension, coral reef environmental health, coastal and estuary water quality, and to help fisheries management (Kahru & Brown, 1997; Miller et al., 2005; Friedl et al., 2006; IOCCG, 2008; and references therein).

However, all these efforts have been dedicated to derive and study the ocean constituents suspended/dissolved in water. On the other hand, algae floating on the water surface, such as the brown macroalgae *Sargassum* spp., have been reported in the literature (e.g., Parr, 1939; Butler & Stoner, 1984; Chernova & Sergeeva, 2008) as well as in various local news media. These surface plants are known to provide important habitat (food and shade) for fish, shrimp, crab, and other marine organisms, including several threatened species of turtles (South Atlantic Fishery Management Council, 2002; Witherington & Hirama, 2006), yet their potential relationship with fish populations and larvae transport has not been documented, possibly due to lack of concurrent data. They also play a role in defining ocean productivity and carbon flux (Muraoka, 2004). *Sargassum* is now considered critical and protected marine habitat and its harvesting in some ocean regions is regulated to protect the associated marine species (South Atlantic Fishery Management Council, 2002). Some species of floating algae can also be used for human food and phycocolloid production (Zemke-White & Ohno, 1999). Conversely,

* Tel.: +1 727 5533987.
E-mail address: hu@marine.usf.edu.

0034-4257/$ – see front matter © 2009 Elsevier Inc. All rights reserved.
doi:10.1016/j.rse.2009.05.012

excessive amount of floating algae in coastal oceans can cause significant adverse impact on local environments and economy, such as the extensive and long-lasting bloom of the green macroalgae *Enteromorpha prolifera* in the Yellow Sea (China) between May and August 2008 (Hu & He, 2008). Dead algae washed onto the beaches must be physically removed in a prompt fashion, and represents an economic burden to local management. Timely information on the size and location of the floating algae is important to help understand fish ecology and to help make management plans. Until recently, however, nearly all reports of these surface organisms are from *in situ* observations that are limited in both space and time, and detection of floating algae from space has been rare.

Gower et al. (2006) first used 300-m full-resolution (FR) MERIS (Medium Resolution Imaging Spectroradiometer, 2002–present) data and 1-km resolution MODIS (Moderate Resolution Imaging Spectroradiometer, 1999–present for Terra, 2002–present for Aqua) data to show the extensive surface slicks, thought to be *Sargassum* spp. (brown or dark-green macro algae), in the Gulf of Mexico (GOM). However, MERIS FR data are available for only limited regions in the world (primarily European waters), and the MODIS 1-km data lack spatial resolution to detect small-scale floating algae. Furthermore, the algorithms used to detect these surface features are not specific to floating algae. While the MCI (Maximum Chlorophyll Index, Gower et al., 2005) is useful in detecting the reflectance peak at 709-nm due to the combined effect of chlorophyll-*a* absorption and fluorescence as well as particulate backscattering, high MCI values can be caused by algae floating on the surface or suspended in the water column, or by sediment plumes. Therefore, the MERIS reflectance spectra from the visible to the near-IR as well as the spatial contrast were examined to distinguish the two types of blooms (Gower et al., 2006). Without referencing the nearby water or examining the full spectral shape, the spatial shape of the detected feature was used to confirm the presence of these surface plants, as floating algae often form thin slicks following wind and currents.

Recently, using the MCI algorithm and MERIS data at reduced resolution (RR, ~1.2 km per pixel), Gower and King (2008) provided the first systematic assessment of *Sargassum* distributions in the GOM and North Atlantic Ocean. Global applications of MCI and MERIS RR data to detect other phytoplankton blooms have also been reported (Gower et al., 2008). Due to the relatively coarse resolution and narrow swath width (~1150 km) of MERIS, small algae slicks might have been missed, which could create errors in understanding their origin, initiation, and distribution statistics.

The MODIS instruments are equipped with several "sharpening" bands designed for land and atmospheric applications with 250-m and 500-m resolutions. Specifically, the 645- and 859-nm bands are 250-m resolution, and the 469-, 555-, 1240-, 1640-, and 2130-nm bands are 500-m resolution. Further, the two MODIS instruments onboard Terra (1999–present) and Aqua (2002–present) satellites with swath widths of 2300 km and equatorial crossing times of 10:30 am and 1:30 pm, respectively, provide more frequent and higher-resolution data than MERIS on a global scale. Several pioneering studies have shown that MODIS medium-resolution data (250- and 500-m) provide great potential in monitoring surface oil slicks (Hu et al., 2003, 2009), algal blooms (Kahru et al., 2004), and coastal/estuarine water quality (Hu et al., 2004; Miller & McKee, 2004; Chen et al., 2007). Large-scale applications of MODIS medium-resolution data in the global ocean to study algae blooms, however, could not been found in the literature. Hu and He (2008) first used these data to study floating algae in the Yellow Sea, yet the simple method used in the study suffered from several problems (see below).

Here, a Floating Algae Index (FAI) is introduced for mapping floating algae in various aquatic environments, the concept of which can be applied to several existing and planned satellite instruments. First, traditional methods to map surface vegetation are introduced, followed by model simulations and data comparisons to show the advantages of the FAI concept. Finally, several examples in the Yellow Sea, East China Sea, North Atlantic Ocean, and Gulf of Mexico from MODIS and Landsat-7/ETM+ are presented and discussed. The objective of this work is to demonstrate the FAI concept to help implement targeted mapping and research plans for any region of interest in the global oceans using MODIS and other fine-resolution satellite instruments.

2. Traditional methods for vegetation mapping

In 1973, Rouse et al. introduced the concept of NDVI (Normalized Difference Vegetation Index) using MSS (MultiSpectral Scanner) data from the US NASA's Earth Resources Technology Satellite (ERTS was later renamed as Landsat-1) (Rouse et al., 1973). NDVI is defined as:

$$\mathrm{NDVI} = (R_{\mathrm{NIR}} - R_{\mathrm{RED}}) / (R_{\mathrm{NIR}} + R_{\mathrm{RED}}), \quad (1)$$

where R_{NIR} and R_{RED} are the reflectance in the near-infrared (NIR) and red bands, respectively. The underlying principle is that all forms of vegetation have a sharp increase in the reflectance spectra (the "red edge") near 700 nm. The difference between R_{NIR} and R_{RED} serves as an index of the vegetation density. Normalization against ($R_{\mathrm{NIR}} + R_{\mathrm{RED}}$) can partially remove the atmospheric effects from different measurements. Some published works also reference radiance instead of reflectance, but the principle is the same.

NDVI is related to the photosynthetic capacity and therefore energy absorption of plant canopies (Sellers, 1985; Myneni et al., 1995). Many applications have utilized NDVI for land cover/land use such as mapping global vegetation and land-based primary production. Its application to AVHRR (Advanced Very High Resolution Radiometer) data to study algae blooms in oceanic and inland waters has also been reported (Prangsma & Roozekrans, 1989; Kahru et al., 1993).

The NDVI concept has been applied to MODIS 250-m resolution data to study the origin and evolution of a massive bloom of the floating algae *E. prolifera* in the Yellow Sea that posed severe management problems for the 2008 Olympic sailing games (Hu & He, 2008). The NDVI method was useful in delineating floating algae from nearby waters. However, NDVI values of both the floating algae and nearby waters are sensitive to variable environmental and observing conditions such as aerosols and solar/viewing geometry. These variable conditions create difficulties in visualization and quantitative analysis since they affect not only the visual contrast between floating algae and nearby waters in the NDVI imagery but change their absolute NDVI values as well. Consequently, interactive color stretching and manual delineation of the region of interest are often required (Hu & He, 2008), making it difficult to implement routine applications to large regions such as the Yellow Sea and East China Sea. In the GOM, MODIS 250-m NDVI images have been found to be able to detect floating algae slicks, thought to be *Sargassum*, but the same limitation apply.

Similar problems have also been found for land vegetation mapping, as NDVI suffers from atmospheric effects, thin clouds, and is also sensor dependent (Holben 1986; Trishchenko et al., 2002). Several modified indexes have been proposed to overcome these difficulties. These include the EVI (Enhanced Vegetation Index) that was designed to strengthen the vegetation signal in high biomass regions and to reduce atmosphere influences. EVI is defined as (Huete & Justice, 1999):

$$\mathrm{EVI} = G \times (R_{\mathrm{NIR}} - R_{\mathrm{RED}}) / (R_{\mathrm{NIR}} + C_1 \times R_{\mathrm{RED}} - C_2 \times R_{\mathrm{BLUE}} + C_3), \quad (2)$$

where G is the gain factor, and C_1, C_2, and C_3 are the pixel-independent coefficients to compensate for aerosol effects and vegetation background, respectively. For MODIS data, $G = 2.5$, $C_1 = 6$, $C_2 = 7.5$, and $C_3 = 1$ (Huete & Justice, 1999).

MODIS EVI was derived using the 469-nm, 645-nm, and 859-nm bands as R_{BLUE}, R_{RED}, and R_{NIR}, respectively, and applied to study the floating algae bloom described in Hu and He (2008). However, the unpublished results showed deficiencies similar to those found with NDVI, i.e., EVI results are also sensitive to the variable environmental and observing conditions. Application of MODIS 250-m NDVI and EVI to detect floating algae, thought to be *Sargassum*, in the GOM suffered from similar problems. Clearly, a better, more efficient method is needed to detect and study these subtle surface features if routine applications to the global oceans are desired.

3. MODIS Floating Algae Index (FAI)

In contrast to land surfaces, water strongly absorbs light in the RED-NIR-SWIR (short-wave infrared) wavelengths. Indeed, due to this high absorption, water is opaque or "black" in the SWIR wavelengths even in the most turbid environments; this provides the basis for using these wavelengths to correct for the atmospheric effects (e.g., Wang & Shi, 2005). On the other hand, algae floating on the water surface have higher reflectance in the NIR than in other wavelengths, and can be easily distinguished from surrounding waters. Fig. 1 shows several MODIS RGB "true-color" composite images for the offshore and coastal waters near Qingdao (China) under various environmental conditions. The spectral reflectance of visually identified floating algae (after interactive color stretching) and their surrounding waters are presented in Fig. 2. In this analysis, MODIS data were first corrected by removing the molecular (Rayleigh) scattering effects, and then converted to Rayleigh-corrected reflectance (R_{rc}) by Hu et al. (2004):

$$R_{rc} = \pi L_t^* / (F_0 \cos\theta_0) - R_r, \tag{3}$$

where L_t^* is the calibrated sensor radiance after adjustment for ozone and other gaseous absorption, F_0 is the extraterrestrial solar irradiance at data acquisition time, θ_0 is the solar zenith angle, and R_r is Rayleigh reflectance estimated with 6S (Vermote et al., 1997). R_{rc} at 645, 555, and 469 nm were used as the R, G, B channels to compose the images in Fig. 1.

Figs. 1 and 2 show that compared with those of the surrounding waters, the R_{rc} spectra of floating algae have a distinguishable peak at 859 nm. This contrast remains even under conditions of the most turbid atmosphere (Figs. 1b and 2b) or significant sun glint (Figs. 1c and 2c). Note that these pixels will be treated as clouds by most cloud-screening algorithms because their R_{rc}(SWIR) values are higher than 3% (Wang & Shi, 2006). Hence, the existing data processing algorithms are not applicable here.

Fig. 2 suggests that the difference between $R_{rc}(859)$, and a baseline between 645-nm and one of the SWIR bands, can be used to detect floating algae. Therefore, the Floating Algae Index is defined as:

$$\begin{aligned} &\mathrm{FAI} = R_{rc,NIR} - R'_{rc,NIR}, \\ &R'_{rc,NIR} = R_{rc,RED} + \left(R_{rc,SWIR} - R_{rc,RED}\right) \times (\lambda_{NIR} - \lambda_{RED}) / (\lambda_{SWIR} - \lambda_{RED}), \end{aligned} \tag{4}$$

where $R'_{rc,NIR}$ is the baseline reflectance in the NIR band derived from a linear interpolation between the red and SWIR bands. Note that the definition of FAI is similar to that for MODIS FLH (Fluorescence Line Height, Letelier & Abott, 1996) and MERIS MCI (Gower et al., 2005), but uses different band combination. In the above equations for MODIS, $\lambda_{RED} = 645$ nm, $\lambda_{NIR} = 859$ nm, $\lambda_{SWIR} = 1240$ nm. The choice of $\lambda_{SWIR} = 1240$ nm instead of 1640 or 2130 nm is based on the fact that for clear atmospheres, $\lambda_{SWIR} = 1240$ nm would lead to a lower baseline and a higher FAI value, which is closer to the "truth" ("truth" defined as the difference between the "Algae" pixel and the nearby "Water" pixel in Figs. 1a and 2a). Further, the 1640 and 2130 nm bands have lower sensitivity (higher noise) and are more separated from

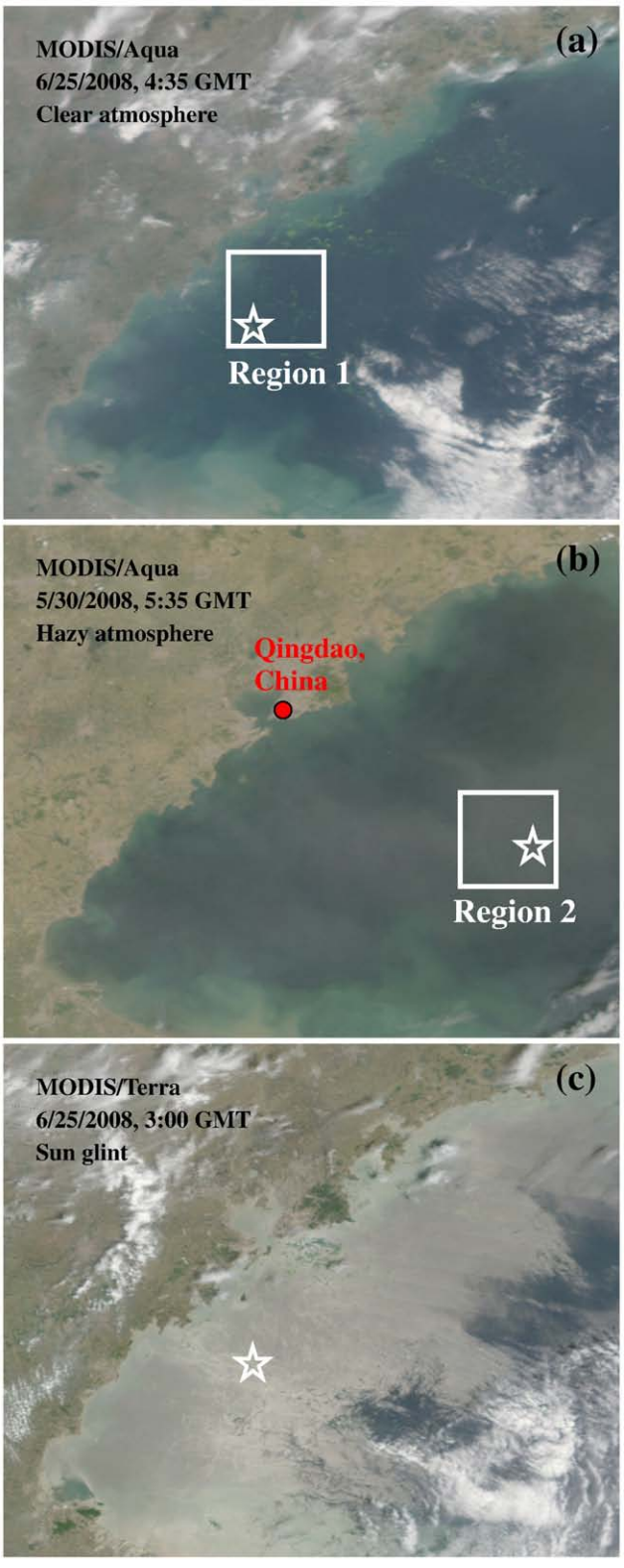

Fig. 1. MODIS 250-m RGB images of the western Yellow Sea near Qingdao, China, where extensive blooms of the floating green macroalgae, *Enteromorpha prolifera*, were found between May and August 2008 (Hu & He, 2008). The images are bound by 34.5°N to 37°N and 119°E to 122°E. The floating algae appear as small green slicks or patches in (a) when the atmosphere is clear, but are barely visible in (b) when the atmosphere is hazy. Image in (c) was collected on the same day as image (a) but contained significant sun glint. The stars mark the locations where reflectance spectra were extracted and analyzed in Fig. 2. Statistics of two regions where floating algae were visually identified through interactive color stretching was generated and presented in Fig. 3. (For interpretation of the references to colour in this figure legend, the reader is referred to the web version of this article.)

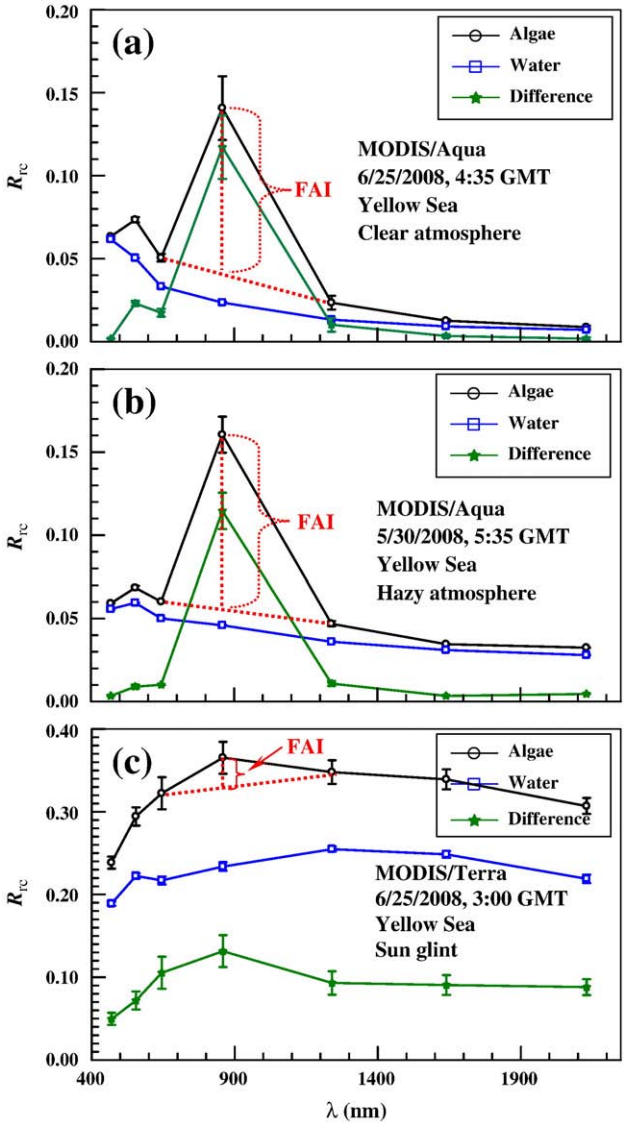

Fig. 2. Rayleigh-corrected MODIS spectral reflectance ($R_{rc}(\lambda)$) of floating algae (circles, with legend "Algae") and nearby water (squares, with legend "Water") on (a) 6/25/2008 4:35 GMT, (b) 5/30/2008 5:35 GMT, and (c) 6/25/2008 3:00 GMT from the locations shown in Fig. 1a, b, and c, respectively. Note that due to strong water absorption at wavelengths > 600 nm, nearly all signals at > 600 nm for the "Water" spectra come from the atmosphere (primarily from aerosols and aerosol–molecule interactions) for this type of sediment-poor water. The atmosphere in (b) is much more turbid (hazy) than in (a), and will be falsely treated as clouds by most cloud detection algorithms. Data in (c) contained significant sun glint, resulting in elevated reflectance across the entire spectra.

645 nm, making interpolation and extrapolation more prone to errors. However, the FAI values calculated using both 1240 and 1640-nm bands showed similar results except that the former resulted in slightly more homogenous background across the MODIS image (>1000 km horizontal scale), suggesting that the 1640-nm band could be used as an alternative in the absence of the 1240-nm band.

4. Sensitivity analysis

A robust index to detect and quantify floating algae must satisfy the following condition: the index over both floating-algae and water pixels should be relatively stable against changing environmental and observing conditions. Fig. 3 shows FAI, NDVI, and EVI values derived from Region 1 and Region 2 outlined in Fig. 1a and b, respectively. Each region contains 180 × 180 image pixels (250-m resolution), which are classified as "algae" and "water" using threshold values obtained from spatial gradient analysis. For the two different atmosphere conditions (clear and hazy), FAI values appear more stable than both NDVI and EVI over both "algae" and "water" pixels. Similar results were obtained for images containing significant sun glint. These results suggest that FAI might be a better index than NDVI and EVI.

Ideally, the comparison should be performed over identical targets under different conditions. In practice, however, this is nearly impossible because of frequent cloud cover and changing locations of the floating algae in two consecutive, cloud-free images. This is why two different regions were chosen to calculate the statistics (mean and standard deviation) in Fig. 3. However, the idealized situation can be simulated using radiative transfer models. To verify and extend the observation in Fig. 3, the sensitivities of the three indexes under various conditions were studied using model simulations in the following way.

Based on the radiative transfer theory and assuming a non-coupling ocean–atmosphere system, R_{rc} can be expressed as

$$R_{rc} = R_a + t_o t R_{target}, \quad (5)$$

where R_a is the aerosol reflectance (including that from the aerosol–molecule interactions), R_{target} is the surface reflectance of the target (either algae or water) as measured from *in situ*, t_o is the atmospheric transmittance from the Sun to the target, and t is the atmospheric transmittance from the target to the satellite sensor. Because floating algae are typically in the form of thin surface slicks due to wind and current (Gower et al., 2006; Hu & He, 2008), t is the beam transmittance for floating algae. In contrast, for the water background, t is the diffuse transmittance.

Two solar/viewing scenarios were considered, with one near satellite nadir (satellite zenith $\theta = 4°$) and the other near the satellite's scan edge ($\theta = 57°$). For each scenario, R_a was estimated using aerosol lookup tables for MODIS (available from SeaDAS data processing software, Baith et al., 2001), for various aerosol types

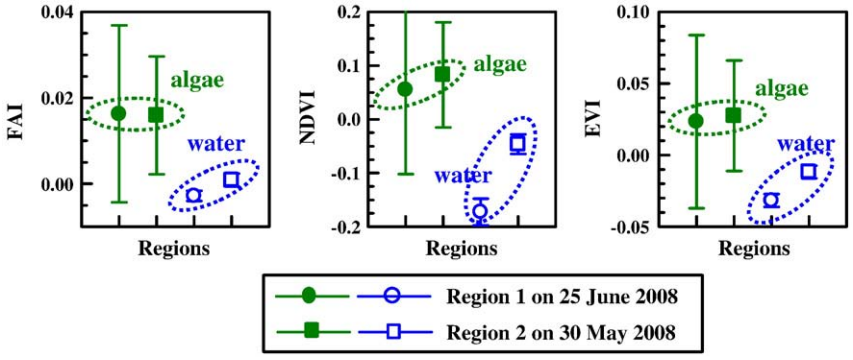

Fig. 3. Mean and standard deviation of various index values over floating algae pixels and water pixels in two regions of the Yellow Sea, outlined in Fig. 1a and b, respectively. Each region contains 180 × 180 MODIS 250-m pixels, with 6699 and 9117 pixels classified as floating algae for the two regions, respectively. FAI values over both algae and water pixels appear more stable than NDVI and EVI for the changing atmospheric and observing conditions.

(maritime, coastal, and troposphere aerosols) and optical thickness, $\tau_a(869)$, between 0.03 and 0.4. The former represents the clearest atmosphere, while the latter is for turbid atmosphere (note that 0.4 exceeds the "high aerosol" flagging threshold used in SeaDAS processing, Robinson et al., 2003).

Fig. 4 shows an example of the sensitivity modeling results. Even for the worse case scenario (i.e., scene edge, $\tau_a(869)=0.4$), FAI(algae) decreased by only 50%, while NDVI(algae) and EVI(algae) decreased by about 70%. For the same solar/viewing geometry, FAI(algae) values for different aerosol types were nearly identical, while NDVI(algae) and EVI(algae) showed noticeable changes. Further, NDVI(water) and EVI(water) changed dramatically (note the discontinuity between solid circles and solid squares) with different aerosol types, $\tau_a(869)$, and solar/viewing geometry, while FAI(water) remained relatively stable. Simulations with other aerosol types showed similar results. Clearly, under all circumstances, FAI is the most stable index among the three for both algae and water pixels, and therefore serves as a better index than NDVI and EVI to detect and map floating algae in the ocean.

The simulation results are consistent with the limited MODIS observations shown in Fig. 3, and further confirmed by comparing the three indexes from imagery with known floating algae under different conditions. Fig. 5 shows an example where FAI and NDVI images, under clear atmosphere, hazy atmosphere, and sun glint, are compared side by side. The FAI images revealed a near-homogeneous background over water pixels in both space and time, over which floating algae pixels could be easily visualized and delineated for further quantification. In contrast, the NDVI images showed more variability in both the image background (water) and target (algae), making them more difficult to differentiate from each other, especially across large spatial and temporal scales. Artifacts over thin clouds or cloud edges were also found in the NDVI images, but they were nearly negligible in the FAI images. The EVI images showed some improvement over the NDVI images, but they also showed more sensitivity than the FAI images to the changing environmental and observing conditions. Indeed, the FAI algorithm removed most of the atmospheric effects and resulted in a relatively homogeneous background from which the outstanding algae (*E. prolifera*) slicks can be clearly visualized. Even under significant sun glint (glint reflectance $L_g>0.02$ sr^{-1}, see right-side of the lower right panel), the FAI image still removed most of the atmospheric effects, resulting in a near-homogenous background. Because of frequent sun glint in tropical and subtropical regions (MODIS instruments do not tilt to avoid sun glint), the ability of FAI to detect floating algae under sun glint can increase spatial and temporal coverage in time-series analysis.

In summary, FAI is a better index than NDVI and EVI primarily due to its relative stability measured across changing environmental and observing conditions. Indeed, the baseline subtraction method provides a simple yet effective means to remove the atmospheric effects, resulting in a quasi inherent optical property (IOP), the FAI. This is particularly useful when large areas (often >1000 km in one direction) are examined, or where environmental conditions may change dramatically across the image.

5. Global examples

The FAI algorithm was implemented to process MODIS data for several selected regions. Specifically, MODIS Level-0 data were obtained from the U.S. NASA GSFC (Goddard Space Flight Center), and processed using SeaDAS5.1 to generate Level-1b data (calibrated radiance). The Level-1b data were corrected for ozone/gaseous absorption and Rayleigh scattering using computer programs from the MODIS Rapid Response Team, and then mapped to a cylindrical equidistance (rectangular) projection using computer programs developed in-

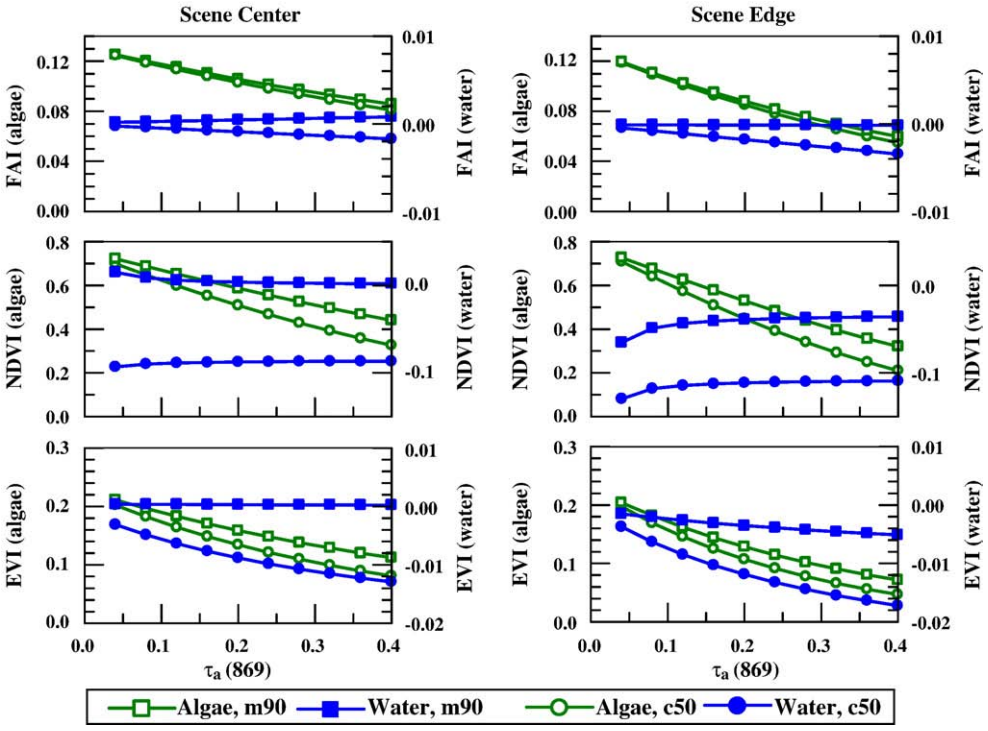

Fig. 4. Sensitivity of FAI, NDVI, and EVI over floating algae ("Algae") and ocean water ("Water") to atmospheric conditions (aerosol type and optical thickness) and solar/viewing geometry, based on model simulations. Figure legend applies to all panels. In this example, two aerosol types typical for the open and coastal oceans are shown: maritime aerosol with 90% relative humidity (m90) and coastal aerosol with 50% relative humidity (c50). $\tau_a(869)$ is the aerosol optical thickness at 869 nm. The left-column panels show the cases near scene center (satellite zenith $\theta=4°$, solar zenith $\theta_0=18.4°$, relative azimuth $\phi=22°$), and the right-column panels are for scene edge ($\theta=57°$, $\theta_0=29°$, $\phi=21°$). Note the changing scales on the *y*-axis. FAI for both "Algae" and "Water" shows the least sensitivity (i.e., most stable) to these changing conditions, as compared with NDVI and EVI. This is especially true for "Water" pixels whose NDVI and EVI values can change dramatically from one aerosol type to another (discontinuity from solid circles to solid squares).

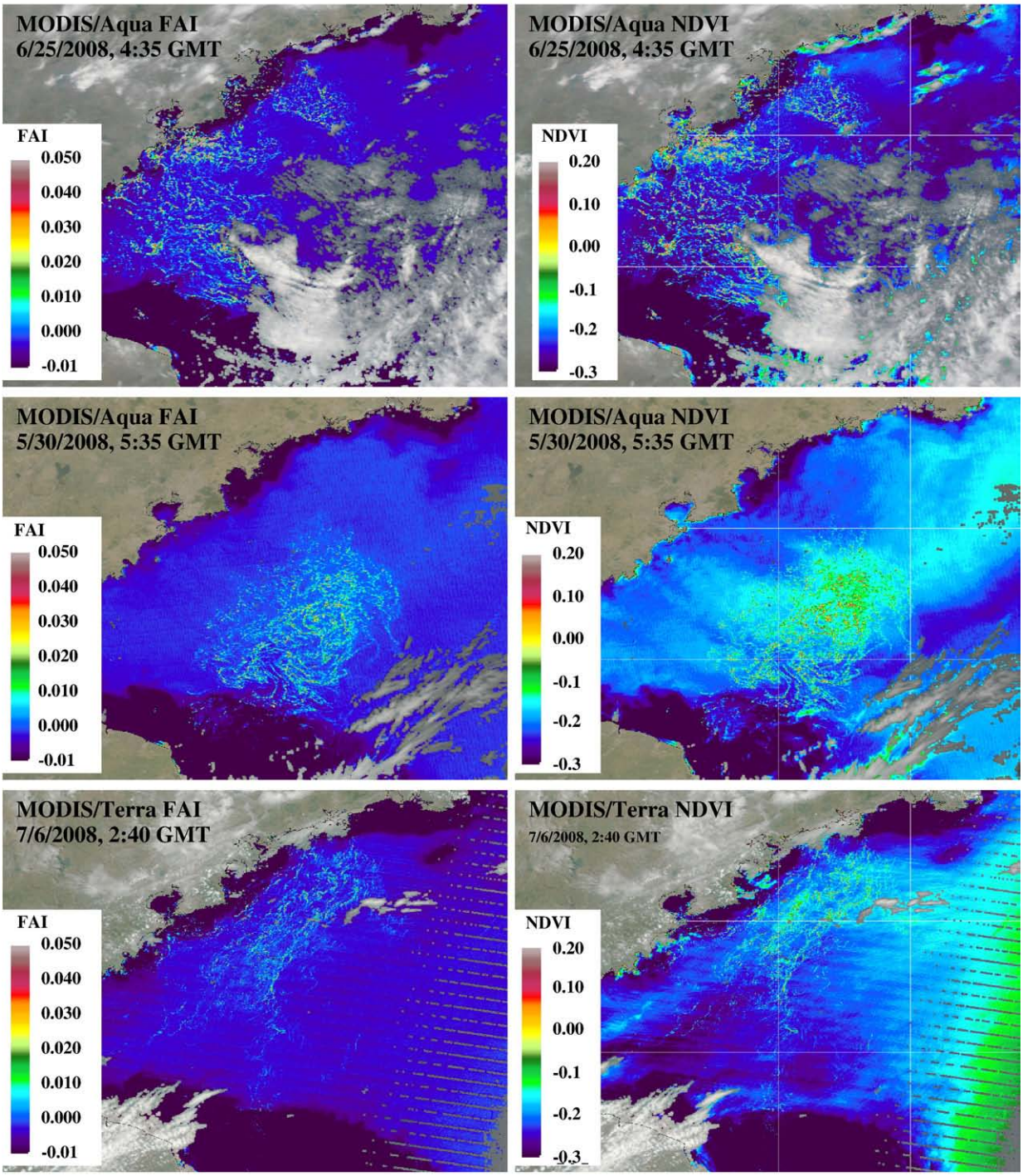

Fig. 5. Comparison between MODIS FAI images (left panels) and NDVI images (right panels) over the Yellow Sea in detecting the floating algae under various environmental and observing conditions. The outstanding slicks are the green macroalgae, *Enteromorpha prolifera*, floating on the water surface. Consistent with the simulation results (Fig. 4), FAI values over both algae and water are more stable than NDVI values, with the latter showing large changes both spatially and temporally. Most of the artifacts in the NDVI images near cloud edges and under sun glint (right side of the lower right panel) are removed in the FAI images. Note that the NDVI image on 6/25/2008 (upper right panel) was used in Hu and He (2008) to show floating algae distribution. More results and comparison can be found under http://www.imars.usf.edu/papers/qingdao_algae/.

house. These map-projected reflectance data were used to derive the FAI images, as defined in Eq. (4).

In theory, the processing could be applied to the entire global ocean dataset. In practice, however, due to the large volume of MODIS data (e.g., a 5-minute MODIS Level-0 granule is about 300–500 MB in size), several regions were selected to demonstrate how FAI could be used to study the spatial/temporal distributions of floating algae. In particular, the examples below show that some of the FAI-identified floating algae have never been observed in satellite imagery or even reported in the peer-reviewed literature, suggesting that applications of the FAI algorithm in the various global oceans using satellite data from MODIS and other instruments may provide unprecedented information on these ecologically important surface features.

5.1. Floating algae off Qingdao, China

Between May and August 2008, significant blooms of the green macroalgae *E. prolifera* were found in the Yellow Sea. The algae first

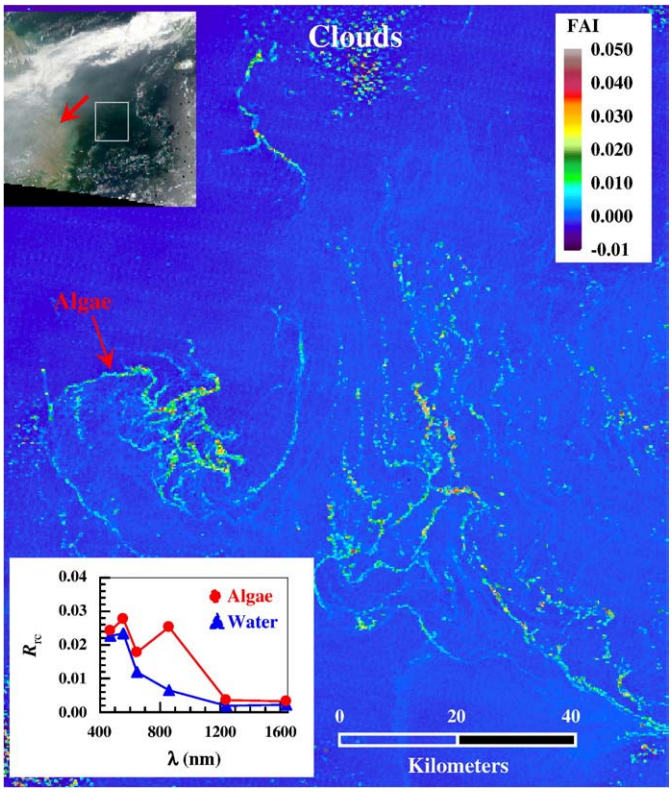

Fig. 6. MODIS/Terra FAI image showing floating algae, thought to be *Enteromorpha prolifera*, on 17 July 2008 in the East China Sea (31°–32.2°N, 123.3°–124.5°E), with location outlined as a rectangular box in the inset MODIS RGB image that covers 29°–35°N and 120°–127°E. The floating algae appear as outstanding thin slicks over near-homogenous background. The image center is about 180 km east of the Yangtze River mouth, annotated with a red arrow in the inset RGB image. The spectral shape (inset figure) of the slick shows a local peak at 859 nm, indicating floating algae instead of foams.

appeared on MODIS imagery on May 14 in the South, then advected to nearshore areas around Qingdao in mid-June (Hu & He, 2008). At least 700,000 tons of algae were collected and buried, yet this only represented a small fraction of the total amount in the ocean. The event lasted for at least two and half months, with the last MODIS image in early August still showing the algae slicks. The event created significant social-economic impact, after which a series of field surveys were conducted to understand the potential causes and consequences (e.g., Lü & Qiao 2008; Sun et al., 2008). In this study, the FAI algorithm (Eq. (4)) was applied to the entire MODIS series used in Hu and He (2008), and improved results, in terms of a more homogenous water background and stable algae–water contrast (as compared with the NDVI images,) were obtained (Fig. 5). Our recent analysis using historical MODIS and Landsat data (Hu et al., submitted for publication-b) showed recurrent algae slicks in the Yellow Sea since 2000, all originated from the nearshore waters of a shallow bank (the Subei Bank) where the seaweed *Porphyra yezoensis* was cultured. The extensive and long-lasting bloom in 2008 was believed to be a direct result of the dramatic expansion of the seaweed aquaculture in 2008. Because these surface algae may recur in the future, the algorithm was implemented using MODIS Level-0 data to routinely generate FAI and RGB imagery for this region. The objective was to provide an early warning system to help local management and coordinate field campaigns.

5.2. Floating algae in the East China Sea

The floating algae slicks shown in Fig. 5 are believed to have been the largest, in terms of area coverage, ever reported for the world's oceans (Hu & He, 2008). At one time, the algae themselves covered an area of ~3800 km^2 in waters of ~23,000 km^2 (Hu & He, 2008). In comparison, although sometimes the western GOM is rich in floating algae (Gower et al., 2006, see below), the algae slicks are much thinner and therefore cover a smaller area. One may wonder whether similar algae slicks of the same type occurred elsewhere in the adjacent oceans during the same time frame. A series of FAI images were generated for the entire Yellow Sea and East China Sea. Results showed that during mid-May of 2008, some surface slicks were found east of the Yangtze River plume. By early June they had developed into extensive slicks about 150–300 km east and northeast of the Yangtze River mouth, and stayed there until at least late July. Fig. 6 shows an example of the slicks identified in this region. Spectral analysis indicated that they had similar spectral shapes as those found in Fig. 5, and a time series analysis together with numerical circulation modeling (Hu et al., submitted for publication-b) suggested that these algae had the same origin as those near Qingdao. Hence, it is very likely that these floating algae are also *E. prolifera*, but the oligotrophic conditions in the central East China Sea led to less intensive blooms. A retrospective analysis using MODIS FAI imagery showed recurrent algae slicks nearly every year since 2000 in this region between April and July (Hu et al., submitted for publication-b). The occurrence of extensive slicks of floating *E. prolifera* in this region could not be found in the peer-reviewed literature, nor in published satellite imagery because all previous studies focused on phytoplankton blooms (including the toxic red tides) and not on floating macroalgae. For example, the cover image of Gower et al. (2008) showed a

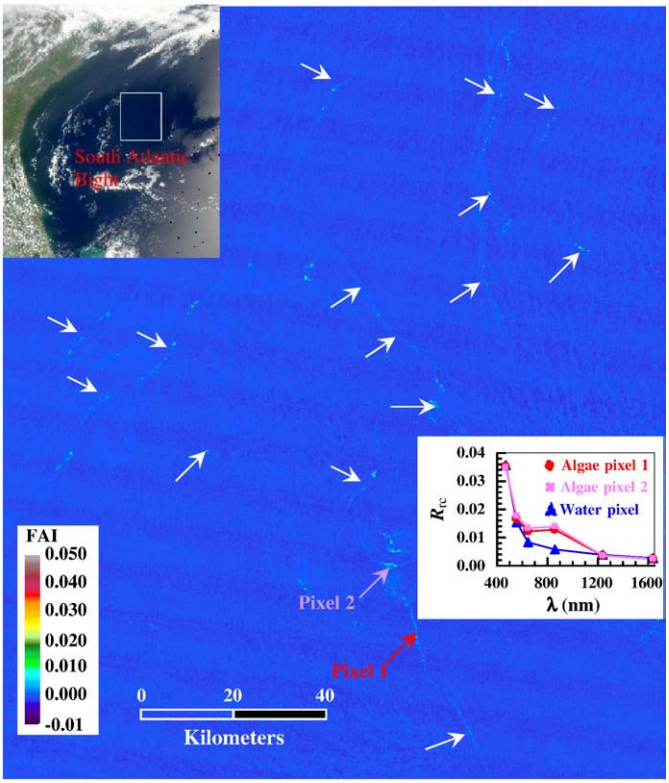

Fig. 7. MODIS/Terra FAI image on 28 May 2008 showing surface slicks, thought to be *Sargassum*, in the South Atlantic Bight bound by 27°–35°N and 82°–74°W (west of the Sargasso Sea in the North Atlantic Ocean, see inset figure). Unlike other atmospheric features, they are static on the MODIS/Aqua FAI image 3 h later on the same day. Further, the spectra of these slicks (inset figure) show apparent reflectance increase at 859 and 645 nm (as compared with nearby "Water" spectrum), indicating surface algae instead of whitecaps or foams. The increase at 645 nm suggests brown rather than green algae, and the features are very likely to be *Sargassum* given that the area is well known to have this marine organism.

bloom patch with high MCI values near the Yangtze River mouth in late July and early August 2006. However, the corresponding MODIS FAI imagery showed no floating algae slicks, suggesting that the high-MCI patch is due to phytoplankton bloom instead of floating macroalgae. Because the latter provides an important habitat for various marine organisms, routine application of the MODIS FAI imagery may provide important information on regional ecology and fisheries.

5.3. Floating algae in the North Atlantic Ocean and Gulf of Mexico

Preliminary results from MODIS FAI showed recurrent surface slicks in the western North Atlantic Ocean and the GOM. An example is presented in Fig. 7, where spectral analysis shows elevated reflectance at 859 and 645 nm (inset figure), suggesting that these thin, outstanding lines may be some sort of macroalgae floating on the water surface. Because *Sargassum* (brown macroalgae) are known to appear in this region and in the Gulf of Mexico (e.g., Gower et al., 2006; Gower & King, 2008), these slicks are very likely to be *Sargassum*. Note that because of the universal color legend used for FAI, the contrast between the algae slicks and the background water is not high in this case, but can be enhanced by interactive color stretching. Compared to slicks in the East China Sea (Fig. 6) and the Yellow Sea (Fig. 5), these slicks are much thinner and farther apart from each other. It is speculated that this difference is primarily due to lack of nutrients in this oligotrophic ocean. Similar thin slicks have also been observed using MODIS FAI imagery in the western GOM (Fig. 8b), in nearshore waters on the shallow west Florida shelf and in the Florida Keys (not shown here), but spatial/temporal statistics will require further analysis. Nevertheless, the example here confirms the effectiveness of 250-m MODIS FAI imagery in detecting floating algae even in the clearest ocean waters.

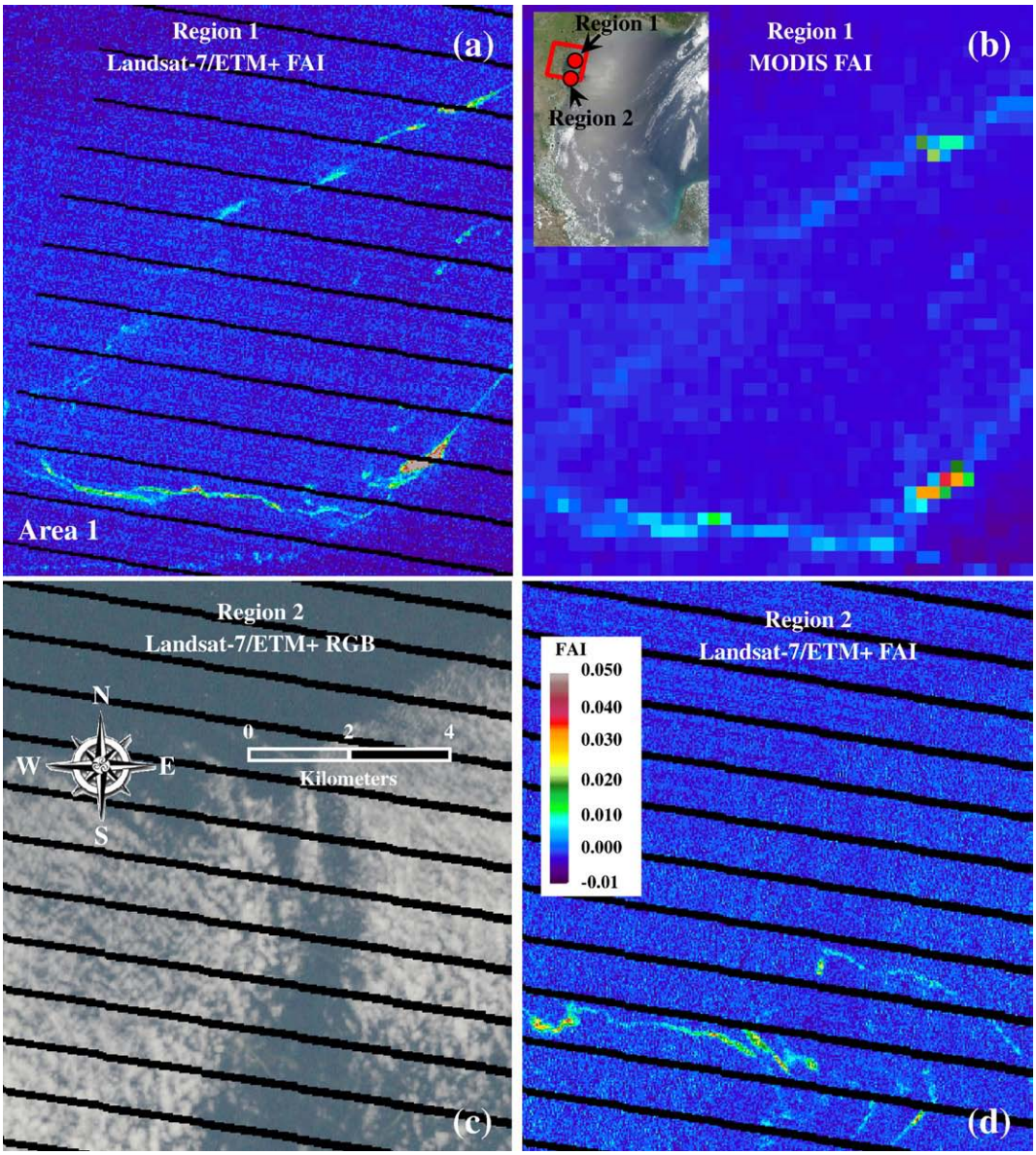

Fig. 8. Landsat-7/ETM+ (30-m resolution) and MODIS/Terra (250-m resolution) imagery within 2 h on 26 April 2007 showing floating algae, thought to be *Sargassum*, in the NW GOM. The inset MODIS RGB image on this day shows significant sun glint in the western GOM (18–30°N, 99–89°W) where the ETM+ coverage is outlined in red. Two small regions of about 11×12 km in size were chosen to show the floating algae, with their locations annotated with two red dots in (b). The FAI images in (a) and (b) show comparison between ETM+ and MODIS for the small region centered at 27.48°N 96.93°W. The ETM+ RGB and FAI images in (c) and (d) are for the small region centered at 26.65°N 96.95°W, where the black lines are due to Scan Line Corrector (SLC) errors. Note that even underneath thin clouds (c), the floating algae slicks, thought be to *Sargassum*, can still be clearly identified using FAI (d).

6. Discussion

6.1. Spatial resolution

Many floating algae slicks can be much smaller than the best MODIS resolution (250-m at satellite nadir, which degrades to 500 m or lower towards satellite scan edge). The ability to detect surface features at sub-pixel scales depends primarily on the feature size (its relative percentage of data contained within the pixel) and satellite sensor sensitivity (signal-to-noise ratio). Fig. 8 shows a comparison between a Landsat/ETM+ sub-image (30-m resolution) and the corresponding MODIS FAI image, co-registered to a rectangular projection. Note that the MODIS sub-image was enlarged to match the Landsat sub-image. In this analysis, Landsat data were processed similarly to MODIS data, with gaseous absorption and Rayleigh scattering corrected first (Eq. (3)), and then mapped to a rectangular projection (Hu et al., 2001). Landsat bands at 660, 825, and 1650 nm were used to derive the Landsat FAI (Eq. (4)), which was then compared to the co-registered MODIS FAI data.

For the area where both Landsat and MODIS have cloud-free data, all slicks identified in the MODIS FAI image appear on the Landsat FAI image, but some slicks can only be identified on the Landsat FAI image because of their small size. The cross-comparison analysis suggests that a surface slick is detectable on the MODIS FAI imagery if its width is at least one fourth of the MODIS pixel size. This corresponds to about 60-m at satellite nadir and 100 to 250-m at satellite scan edge. The comparison also suggests that although Landsat/ETM+ sensitivity is several times lower than the MODIS 250-m detectors (Table 1 in Hu et al., 2004), spatial resolution appears to be the primary limiting factor. The same argument may be applied to MODIS and MERIS. While the MODIS 250-m bands were designed for land/atmosphere studies and therefore have lower sensitivity than MERIS, the increased spatial resolution of MODIS (250-m) from the MERIS RR data (1.2 km) may enhance the our capability to detect and map small algae patches in large water bodies.

Fig. 8 suggests that Landsat data can complement the MODIS findings for small-sized floating algae, even though Landsat coverage is restricted to near-shore waters only (typically within 100–200 km of the coast). Indeed, many Landsat FAI images around Florida Keys revealed extensive thin slicks of floating algae during summer, which are not detectable by the coarser-resolution MODIS FAI images. Similarly, Landsat data over the nearshore waters of the Subei Bank (north of the Yangtze River mouth) showed recurrent thin algae slicks between 2000 and 2008 that are not detectable by MODIS (Hu et al., submitted for publication-b). Such ability of Landsat is particularly useful as global Landsat ETM+ data (1999–present) and TM data (1982–present) are freely available from the United States Geological Survey (USGS). For any targeted coastal regions in the world, the free availability of the long-term MODIS and Landsat data, and the simple FAI algorithm, make implementation of a system to study the spatial/temporal distributions of floating algae straightforward.

6.2. Atmospheric correction

Ideally, surface reflectance (R_{target} in Eq. (5)) should first be derived from the satellite signal by correcting for both Rayleigh scattering (R_r in Eq. (3)) and aerosol effects (R_a in Eq. (5)), with the latter estimated from the satellite measurement over every pixel, and then used as input of the FAI algorithm. Unfortunately, there is currently no reliable atmospheric correction that can be applied to derive R_{target} when the target is floating algae.

The atmospheric correction scheme designed for the ocean assumes negligible water reflectance ("black" pixels) in the NIR (Gordon, 1997) for the open ocean or in the SWIR (Wang & Shi, 2005) for turbid waters. Aerosol contributions to the satellite signal are first estimated in these wavelengths, and then extrapolated to the visible using pre-computed aerosol lookup tables. However, Fig. 2 shows that floating algae, similar to land surface, have non-zero reflectance even in the SWIR. Further, atmospheric correction designed for the ocean regards the surface Fresnel reflection as part of the atmospheric effect instead of the target signal. Hence, this approach is inapplicable for FAI derivation.

Because floating algae are similar to land vegetation, it appears logical to use an atmospheric correction scheme designed for land. The Vermote and Vermeulen (1999) MODIS atmospheric correction scheme, designed for land, takes a similar approach to the ocean atmospheric correction but uses the 6S radiative transfer code (Vermote et al., 1997) to first construct an aerosol lookup table, and then uses the MODIS aerosol products from the Kaufman et al. (1997) algorithm to estimate and remove the aerosol effect. Indeed, the MODIS global surface reflectance products (MOD09GQ and MYD09GQ with sinusoidal projection) based on these algorithms for the 250-m and 500-m bands, are available at the USGS LPDAAC (Land Processes Distributed Active Archive Center). However, there are two problems in using these products to derive FAI. First, the uncertainties in the derived aerosol optical thickness (>0.05 in the blue) and surface reflectance (~1%) are too large for water applications. Second, examination of the products corresponding to those in Fig. 1 showed significant patchiness and also large areas of masked (i.e., unprocessed), but valid, data. Therefore, these products could not be used to derive FAI.

One might further improve these existing algorithms. However, because any sophisticated algorithm will use certain assumptions and information from some spectral bands to derive the aerosol signals in other bands, an over- or under-correction is often inevitable. It is even worse when this type of error changes the sign from positive to negative between adjacent pixels (e.g., from an "algae" pixel to a "water" pixel), creating larger errors in the algae–water contrast. The current FAI algorithm, although simple, is effectively an atmospheric correction to remove most, if not all, of the aerosol effect, as shown in Figs. 2a–b and 5. Indeed, the FAI design is similar to that for MODIS FLH (Fluorescence Line Height, Letelier & Abott, 1996) and MERIS MCI (Gower et al., 2005), both of which provide an effective means to remove atmospheric effects in order to estimate solar-stimulated chlorophyll-*a* fluorescence and to detect intense phytoplankton blooms. Hence, before a robust atmospheric correction algorithm specifically designed for floating algae in the ocean is developed, incorporating the simple FAI algorithm based on Rayleigh-corrected reflectance (Eq. (4)) may be the most practical way to detect and monitor these subtle surface features using a variety of satellite sensors.

6.3. Cloud masking

Cloud pixels show high FAI values, and therefore may be misinterpreted as floating algae if they also appear as thin lines or small patches. It is therefore desirable to overlay a reliable cloud mask on the FAI image to facilitate visual interpretation and quantitative analysis. Unfortunately, there is no existing cloud-masking algorithm that identifies all cloud pixels while keeping all valid algae pixels. The default SeaDAS cloud masking algorithm uses a single threshold of $R_{rc}(869) = 2.7\%$, corresponding to $\tau_a(869) \approx 0.3$ for maritime aerosols. This often masks near-shore turbid water pixels due to significant water signal at this wavelength. A recent improvement (Wang & Shi, 2006) used threshold values in the SWIR wavelengths instead, (namely $R_{rc}(1240) = 2.35\%$ and $R_{rc}(1640) = 2.15\%$), but unfortunately it too will falsely identify the hazy atmosphere (Figs. 1b and 2b) as clouds, resulting in loss of valid data. The most confounding problem, however, is to mask clouds but keep the sun glint "contaminated" pixels because useful information can still be extracted from sun glint pixels (Figs. 1c, 2c, and 5). The threshold approaches simply do not

work because both cloud and glint pixels show high $R_{rc}(1240)$ values (>3.0%). Several sophisticated cloud and glint detection algorithms rely either on light polarization properties (Lotz et al., 2008) or the thermal bands, as in the MODIS cloud masking algorithm (Frey et al., 2008). Further, the threshold values for these algorithms may vary with space and time (Jedlovec et al., 2008). Consequently, the cloud mask generated using the 1-km resolution thermal bands (during SeaDAS processing of MODIS data) often masks some of the glint area or the algae pixels, and therefore cannot be applied operationally.

An attempt has been made to use not only the $R_{rc}(1240)$ threshold but also the spectral shape of R_{rc} between 469 and 2130 nm to differentiate clouds and sun glint, with the underlying principle that clouds are spectrally flat (i.e., white) but sun glint is red rich (i.e., blue-light is scattered out of the satellite field of view with relatively more red light reaching the satellite sensor). Limited success has been achieved (Fig. 5), but the parameterization may be fine tuned with more datasets in future work. The added convenience for visual examination and statistical analysis, however, is at the price of added complexity in processing and requirement of more spectral bands. Even without these additional steps, cross-examination of the FAI and RGB image pair can easily rule out clouds and identify the various features.

6.4. Continuity considerations

The FAI concept can be applied to any satellite sensor that is equipped with three spectral bands in the red, NIR, and SWIR at medium resolution (<500 m per pixel). For example, the Japanese Global Imager (GLI) onboard the ADEOS-II (December 2002–October 2003) is equipped with six 250-m "sharpening" bands at 460, 545, 660, 825, 1640, 2210 nm, respectively, where FAI can be derived from the 660, 825, and 1640-nm bands. Most importantly, the next generation of low Earth-orbiting environmental satellites, namely the NPOESS (National Polar-orbiting Operational Environmental Satellite System), will be equipped with sensors similar to MODIS. For example, VIIRS (Visible Infrared Imager/Radiometer Suite), the ocean color sensor on the NPP (NPOESS Preparatory Project) mission (satellite to be launched in 2009), has three imaging bands at 640, 865, and 1610 nm at medium resolution (371×387 m nadir, 800×789 m scan edge). These bands are perfectly suitable to derive a VIIRS FAI, similar to the MODIS FAI, assuring not only continuity but comparability after MODIS. Similarly, the next-generation of Landsat-like high-resolution sensor has been designed for the Landsat Data Continuity Mission (LDCM) which is planned for launch by 2011, and will allow for a LDCM FAI to be derived similar to that for Landsat (Fig. 8). In the meantime, the free availability of global Landsat TM/ETM+ data provide an excellent data source to study small-scale (10–100 m) floating algae in the global coastal zones.

6.5. Other applications

The FAI design examines the reflectance peak in the NIR; therefore, any surface vegetation in aquatic environment can be detected. Certain cyanobacteria species are known to be able to adjust their buoyancy, making them appear as surface vegetation; in calm weather they can form surface or subsurface mats instead of being uniformly mixed with water (Paerl & Ustach, 1982; Sellner, 1997). The cyanobacteria blooms of the blue-green algae *Microcystis aeruginosa* in Taihu Lake, China, for example, occurred every year in the past decade and sometimes caused significant social-economic impact (Guo, 2008). An attempt is currently underway to establish a long-term series of intense blooms using the FAI method and MODIS 250-m and 500-m data between 2000 and 2008. The results show spatial/temporal bloom characteristics that were previously unknown but agree with other water quality measurements (Hu et al., submitted for publication-a).

Indeed, using satellite remote sensing to study cyanobacteria blooms is not new. For example, Kahru et al. (2007) combined the green-red bands from satellite data from CZCS (Coastal Zone Color Scanner, 1978–1986), SeaWiFS (Sea-viewing Wide Field-of-view Sensor, 1997–), and MODIS/Aqua, to establish a long-term time series (1979–1984, 1998–2006) of cyanobacteria blooms of *N. spumigena* in the Baltic Sea. To the author's knowledge this is the only long-term record of cyanobacteria blooms in a marginal sea based on satellite data alone. Preliminary results from application of MODIS FAI imagery to the Baltic Sea showed that MODIS FAI was effective only when the cyanobacteria formed thick mats, suggesting that MODIS FAI may not be used directly for that region. However, the classification method using green-red bands (Kahru et al.) is sensitive to suspended sediments and environmental conditions (e.g., haze, sun glint). FAI, in contrast, is relatively insensitive to these variable conditions. For example, FAI values in sediment-rich waters are negative, and they decrease with increasing sediment concentrations, making these waters well distinguishable from those containing floating algae. The higher resolution of MODIS data (250-m) is more desirable than the traditional 1-km resolution of CZCS and SeaWiFS for small water bodies. It remains to be studied, however, on how to integrate MODIS FAI with other satellite data products to improve water quality estimates in the Baltic Sea and other similar water bodies with known cyanobacteria blooms. Likewise, and in a more general extent, whether or not MODIS and Landsat FAI can be used for land vegetation mapping should also be tested in the future.

7. Conclusion

A simple ocean color index is introduced here to detect various floating algae in the global oceans. The FAI (Floating Algae Index), defined as the difference between Rayleigh-corrected reflectance in the NIR and a baseline formed by the red and SWIR bands, is an effective index to detect surface vegetation in the ocean by removing most of the atmospheric effects. Data comparison and model simulations showed that FAI is more advantageous than the traditional NDVI or EVI because FAI is less sensitive to changes in environmental and observing conditions such as aerosols and solar/viewing geometry. Application of FAI imagery derived from MODIS and Landsat-7/ETM+ in a variety of environments showed success in mapping floating algae even under significant sun glint or thin clouds. Because of the availability of the three spectral bands in the existing and planned high-resolution and medium-resolution satellite sensors (Landsat-4/TM, Landsat-5/TM, Landsat-7/ETM+, MODIS/Aqua, MODIS/Terra, VIIRS/NPP, LDCM), and also because of the free availability of global MODIS and Landsat data, FAI could be used as a reliable index in establishing a long-term record of floating algae distributions in any part of the global oceans.

Acknowledgement

This work was supported by the U.S. NASA (NNS04AB59G, NNX09AE17G) and NOAA (NA06NES4400004). MODIS data were provided by the NASA Goddard Space Flight Center (http://oceancolor.gsfc.nasa.gov). The constructive comments from three anonymous reviewers are greatly appreciated.

References

Alvain, S., Moulin, C., Dandonneau, Y., & Breon, F. M. (2005). Remote sensing of phytoplankton groups in case 1 waters from global SeaWiFS imagery. *Deep-Sea Research*, *52*, 1989−2004.

Austin, R. W., & Petzold, T. J. (1981). The determination of the diffuse attenuation coefficients of sea water using the coastal zone color scanner. In J. F. R. Gower (Ed.), *Oceanography from space* (pp. 239−256). New York: Plenum.

Baith, K., Lindsay, R., Fu, G., & McClain, C. R. (2001). Data analysis system developed for ocean color satellite sensors.*EOS, American Geophysical Union Transactions*, *82*(18) (1 May 2001).

Brown, C. W., & Yoder, J. A. (1994). Coccolithophorid blooms in the global ocean. *Journal of Geophysical Research*, *99*, 7467−7482.

Butler, J. N., & Stoner, A. W. (1984). Pelagic Sargassum: Has its biomass changed in the last 50 years? *Deep-Sea Research*, *31*, 1259−1264.

Cannizzaro, J. P., Carder, K. L., Chen, F. R., Heil, C. A., & Vargo, G. A. (2008). A novel technique for detection of the toxic dinoflagellate, Karenia brevis, in the Gulf of Mexico from remotely sensed ocean color data. *Continental Shelf Research*, *28*, 137−158.

Chen, Z., Hu, C., & Muller-Karger, F. E. (2007). Monitoring turbidity in Tampa Bay using MODIS/Aqua 250-m imagery. *Remote Sensing of Environment*, *109*, 207−220.

Chernova, E. N., & Sergeeva, O. S. (2008). Metal concentrations in Sargassum algae from coastal waters of Nha Trang Bay (South China Sea). *Russian Journal of Marine Biology*, *34*, 57−63.

Cullen, J. J., Ciotti, A. M., Davis, R. F., & Lewis, M. R. (1997). Optical detection and assessment of algal blooms. *Limnology and Oceanography*, *42*, 1223−1239.

Frey, R. A., Ackerman, S. A., Liu, Y., Strabala, K. I., Zhang, H., Key, J. R., et al. (2008). Cloud detection with MODIS. Part I: Improvements in the MODIS cloud mask for Collection 5. *Journal of Atmospheric and Oceanic Technology*, *25*, 1057−1072.

Friedl, L., Wilson, C., Chao, Y., Bograd, S., & Turner, W. (2006). Using satellite data products to manage living marine resources. *Eos, American Geophysical Union Transactions*, *87*(41), 437.

Gordon, H. R. (1997). Atmospheric correction of ocean color imagery in the Earth Observing System era. *Journal of Geophysical Research*, *102*, 17081−17106.

Gordon, H. R., Boynton, G. C., Balch, W. M., Groom, S. B., Harbour, D. S., & Smyth, T. J. (2001). Retrieval of coccolithophore calcite concentration from SeaWiFS imagery. *Geophysical Research Letters*, *28*, 1587−1590.

Gordon, H. R., & Morel, A. (1983). Remote assessment of ocean color for interpretation of satellite visible imagery: A review. *Lecture Notes on Coastal and Estuarine Studies* New York: Springer-Verlag 113 pp. 1983.

Gower, J., Hu, C., Borstad, G., & King, S. (2006). Ocean color satellites show extensive lines of floating Sargassum in the Gulf of Mexico. *IEEE Transactions on Geoscience and Remote Sensing*, *44*, 3619−3625.

Gower, J., & King, S. (2008). Satellite images show the movement of floating Sargassum in the Gulf of Mexico and Atlantic Ocean.*Nature Precedings* (hdl:10101/npre.2008.1894.1).

Gower, J., King, S., Borstad, G., & Brown, L. (2005). Detection of intense plankton blooms using the 709 nm band of the MERIS imaging spectrometer. *International Journal of Remote Sensing*, *26*, 2005−2012.

Gower, J., King, S., & Goncalves, P. (2008). Global monitoring of plankton blooms using MERIS MCI. *International Journal of Remote Sensing*, *29*, 6,209−6,216.

Guo, L. (2008). Doing battle with the green monster of Taihu Lake. *Science*, *317*, 1166.

Holben, B. N. (1986). Characteristics of maximum-value composite images from temporal AVHRR data. *International Journal of Remote Sensing*, *7*, 1417−1434.

Hu, C., Chen, Z., Clayton, T. D., Swarzenski, P., Brock, J. C., & Muller-Karger, F. E. (2004). Assessment of estuarine water-quality indicators using MODIS medium-resolution bands: Initial results from Tampa Bay, Florida. *Remote Sensing of Environment*, *93*, 423−441.

Hu, C., & He, M. -X. (2008). Origin and offshore extent of floating algae in Olympic sailing area. *Eos, American Geophysical Union Transactions*, *89*(33), 302−303.

Hu, C., Lee, Z., Ma, R., Yu, K., Li, D., and Shang, S. (submitted for publication-a). MODIS observations of cyanobacteria blooms in Taihu Lake, China. Journal of Geophysical Research.

Hu, C., Li, D., Chen, C., Ge, J., Muller-Karger, F., He, M-X., et al. (submitted for publication-b). On the origin of the macroalgae *Enteromorpha prolifera* in the Yellow Sea and East China Sea. Journal of Geophysical Research.

Hu, C., Li, X., Pichel, W. G., & Muller-Karger, F. E. (2009). Detection of natural oil slicks in the NW Gulf of Mexico using MODIS imagery. *Geophysical Research Letters*, *36*, L01604. doi:10.1029/2008GL036119

Hu, C., Muller-Karger, F. E., Andrefouet, S., & Carder, K. L. (2001). Atmospheric correction and calibration of LANDSAT-7/ETM+ imagery over aquatic environments: A multi-platform approach using SeaWiFS/MODIS. *Remote Sensing of Environment*, *78*, 99−107.

Hu, C., Muller-Karger, F. E., Taylor, C., Myhre, D., Murch, B., Odriozola, A. L., et al. (2003). MODIS detects oil spills in Lake Maracaibo, Venezuela. *Eos, Transactions American Geophysical Union*, *84*(33), 313, 319.

Huete, A. R., & Justice, C. (1999). MODIS vegetation index (MOD13) algorithm theoretical basis document Ver. 3. 1999.

IOCCG (2005). Ocean-colour bio-optical algorithms. In Z. P. Lee (Ed.), *Reports of the International Ocean-Colour Coordinating Group, No. 5, IOCCG, Dartmouth, Canada*.

IOCCG (2008). Why ocean colour? The societal benefits of ocean-colour technology. In T. Platt, N. Hoepffner, V. Stuart, & C. Brown (Eds.), *Reports of the International Ocean-Colour Coordinating Group, No. 5, IOCCG, Dartmouth, Canada*.

Jedlovec, G., Haines, S. L., & LaFontaine, F. (2008). Spatial and temporal varying thresholds for cloud detection in GOES imagery. *IEEE Transactions on Geoscience and Remote Sensing*, *46*, 1705−1717.

Kahru, M., and Brown, C.W. (1997). Monitoring algal blooms: New techniques for detecting large-scale environmental change. Springer–Verlag and Landes Bioscience, 1997.

Kahru, M., Leppänen, J. M., & Rud, O. (1993). Cyanobacterial blooms cause heating of the sea surface. *Marine Ecology. Progress Series*, *101*, 1−7.

Kahru, M., Mitchell, B. G., Diaz, A., & Miura, M. (2004). MODIS detects a devastating algal bloom in Paracas Bay, Peru. *Eos, Transactions American Geophysical Union*, *85*(45), 465.

Kahru, M., Savchuk, O. P., & Elmgren, E. (2007). Satellite measurements of cyanobacteria bloom frequency in the Baltic Sea: Interannual and spatial variability. *Marine Ecology. Progress Series*, *343*, 15−23.

Kaufman, Y. J., Tanre, D., Remer, L. A., Vermote, E. F., Chu, A., & Holben, B. N. (1997). Operational remote sensing of tropospheric aerosol over land from EOS moderate resolution imaging spectroradiometer. *Journal of Geophysical Research*, *102*(D14), 17051−17067.

Lee, Z. P., Carder, K. L., & Arnone, R. A. (2002). Deriving inherent optical properties from water color: A multiband quasi-analytical algorithm for optically deep waters. *Applied Optics*, *41*, 5755−5772.

Lee, Z. P., Du, K. P., & Arnone, R. (2005). A model for the diffuse attenuation coefficient of downwelling irradiance. *Journal of Geophysical Research*, *110*, C02016. doi:10.1029/2004JC002275.1

Letelier, R. M., & Abott, M. R. (1996). An analysis of chlorophyll fluorescence algorithms for the Moderate Resolution Imaging Spectrometer (MODIS). *Remote Sensing of Environment*, *58*, 215−223.

Lotz, W. A., Vountas, M., Dinter, T., & Burrows, J. P. (2008). Cloud and surface classification using SCIAMACHY polarization measurement devices. *Atmospheric Chemistry and Physical Discussion*, *8*, 9855−9881.

Lü, X., & Qiao, F. (2008). Distribution of sunken macroalgae against the background of tidal circulation in the coastal waters of Qingdao, China, in summer 2008. *Geophysical Research Letters*, *35*, L23614. doi:10.1029/2008GL036084

Maritorena, S., Siegel, D. A., & Peterson, A. R. (2002). Optimization of a semianalytical ocean color model for global-scale application. *Applied Optics*, *41*, 2705−2714.

McClain, C. R., Feldman, G. C., & Hooker, S. B. (2004). An overview of the SeaWiFS project and strategies for producing a climate research quality global ocean bio-optical time series. *Deep-Sea Research II*, *51*, 5−42.

Miller, R. L., Del Castillo, C. E., & McKee, B. A. (2005). Remote sensing of aquatic coastal environments New York: Springer-Verlag 345 pp.

Miller, R. L., & McKee, B. A. (2004). Using MODIS Terra 250 m imagery to map concentrations of total suspended matter in coastal waters. *Remote Sensing of Environment*, *93*, 259−266.

Morel, A., Ahn, Y. H., Partensky, F., Vaulot, D., & Claustre, H. (1993). Prochlorococcus and Synechococcus – A comparative-study of their optical-properties in relation to their size and pigmentation. *Journal of Marine Research*, *51*, 617−649.

Morel, A., & Prieur, L. (1977). Analysis of variations in ocean color. *Limnology and Oceanography*, *22*, 709−722.

Muraoka, D. (2004). Seaweed resources as a source of carbon fixation.*Bulletin of the Fisheries Research Agency*, 59−63 (Supplement No. 1).

Myneni, R. B., Hall, F. G., Sellers, P. J., & Marshak, A. L. (1995). The interpretation of spectral vegetation indexes. *IEEE Transactions on Geoscience and Remote Sensing*, *33*, 481−486.

O'Reilly, J. E., Maritorena, S., O'Brien, M. C., Siegel, D. A., Toole, D., Menzies, D., et al. (2000). SeaWiFS postlaunch calibration and validation analyses: Part 3. In S. B. Hooker, & E. R. Firestone (Eds.), *SeaWiFS postlaunch technical report series, 11NASATechnical Memorandum 2000-206892*. 49 pp.

Paerl, H. W., & Ustach, J. F. (1982). Blue-green algae scum's: An explanation for their occurrence during freshwater blooms. *Limnology and Oceanography*, *27*, 212−217.

Parr, A. E. (1939). Quantitative observations on the pelagic Sargassum vegetation of the western north Atlantic. *Bulletin of the Bingham Oceanographic Collection*, *6*, 1−94.

Prangsma, G. J., & Roozekrans, J. N. (1989). Using NOAA AVHRR imagery in assessing water quality parameters. *International Journal of Remote Sensing*, *10*, 811−818.

Robinson, W. D., Franz, B. A., Patt, F. S., Bailey, S. W., & Werdell, P. J. (2003). *Masks and flags updates.* SeaWiFS Postlaunch Technical Report Series, NASA Tech. Memo. 2003-206892, 2003.

Rouse, J. W., Haas, R. H., Schell, J. A., & Deering, D. W. (1973). Monitoring vegetation systems in the Great Plains with ERTS. *Third ERTS Symposium, NASA SP-351 I* (pp. 309−317).

Sathyendranath, S., Prieur, L., & Morel, A. (1989). A three component model of ocean colour and its application to remote sensing of phytoplankton pigments in coastal waters. *International Journal of Remote Sensing*, *10*, 1373−1394.

Sathyendranath, S., Watts, L., Devred, E., Platt, T., Caverhill, C., & Maass, H. (2004). Discrimination of diatoms from other phytoplankton using ocean-colour data. *Marine Ecology. Progress Series*, *272*, 59−68.

Sellers, P. J. (1985). Canopy reflectance, photosynthesis, and transpiration. *International Journal of Remote Sensing*, *6*, 1335−1372.

Sellner, K. G. (1997). Physiology, ecology and toxic properties of marine cyanobacteria blooms. *Limnology and Oceanography*, *42*, 1089−1104.

South Atlantic Fishery Management Council (2002). *Fishery management plan for pelagic Sargassum habitat of the South Atlantic region* http://www.safmc.net/library/sargFMP.pdf

Subramaniam, A., Brown, C. W., Hood, R. R., Carpenter, E. J., & Capone, D. G. (2002). Detecting Trichodesmium blooms in SeaWiFS imagery. *Deep-Sea Research II*, *49*, 107−121.

Sun, S., Wang, F., Li, C., Qin, S., Zhou, M., Ding, L., et al. (2008). Emerging challenges: Massive green algae blooms in the Yellow Sea. *Nature Precedings* (hdl:10101/npre.2008.2266.1).

Trishchenko, A. P., Cihlar, J., & Li, Z. -Q. (2002). Effects of spectral response function on surface reflectance and NDVI measured with moderate resolution satellite sensors. *Remote Sensing of Environment*, *81*, 1−18.

Vermote, E. F., Tanre, D., Deuze, J. L., Herman, M., & Morcette, J. -J. (1997). Second simulation of the satellite signal in the solar spectrum, 6S: An overview. *IEEE Transactions on Geoscience and Remote Sensing*, *35*, 675−686.

Vermote, E. F., & Vermeulen, A. (1999). Atmospheric correction algorithm: Spectral reflectances (MOD09). *MODIS Algorithm Theoretical Background Document, version 4.0* (http://modis.gsfc.nasa.gov/data/atbd/atbd_mod08.pdf).

Wang, M., & Shi, W. (2005). Estimation of ocean contribution at the MODIS near-infrared wavelengths along the east coast of the U.S.: Two case studies. *Geophysical Research Letters*, *32*(13), L13106. doi:10.1029/2005GL022917

Wang, M., & Shi, W. (2006). Cloud masking for ocean color data processing in the coastal regions. *IEEE Transactions on Geoscience and Remote Sensing*, *44*, 3196−3205.

Witherington, B., and Hirama, S., (2006). Sea turtles of the epi-pelagic Sargassum drift community. In M. Frick, A. Panagopoulou, A. F. Rees, & K. Williams (Compilers). Book of Abstracts. Twenty Sixth Annual Symposium on Sea Turtle Biology and Conservation. International Sea Turtle Society, Athens, Greece. P. 209.

Yentsch, C. S. (1960). The influence of phytoplankton pigments on the colour of seawater. *Deep-Sea Research*, *7*, 1−9.

Yentsch, C. S. (1983). Remote sensing of biological substances. In A. P. Cracknell (Ed.), *Remote Sensing Applications in Marine Science and Technology* (pp. 263−297). D. Reidel Publishing Company.

Zemke-White, W. L., & Ohno, M. (1999). World seaweed utilisation: An end-of-century summary. *Journal of Applied Phycology*, *11*, 369−376.